Anharmonic dynamics in crystalline, glassy, and supercooled-liquid glycerol: A case study on the onset of relaxational behavior

G. J. Cuello, F. J. Bermejo, R. Fayos, R. Fernández-Perea, and A. Criado
Consejo Superior de Investigaciones Científicas, Serrano 123, Madrid E-28006, Spain

F. Trouw and C. Tam
Argonne National Laboratory, Argonne, Illinois 60439-4815

H. Schober
Institut Laue Langevin, Boîte Postale 156x, F-38042 Grenoble Cedex 9, France

E. Enciso and N. G. Almarza
Departamento de Química-Física I, Universidad Complutense, Madrid, E-28040, Spain
(Received 5 August 1997; revised manuscript received 22 October 1997)

The temperature dependence of the spectral distributions of the glass, crystalline, and supercooled-liquid phases of glycerol is investigated by means of neutron inelastic scattering. The importance of anharmonic effects is quantified by the temperature dependence of reduced spectral frequency moments. The onset of relaxational (i.e., stochastic, zero-frequency) motions in the supercooled liquid state is monitored by neutron quasielastic scattering. A substantial deviation of the observed linewidths from the hydrodynamic prescription is observed and is interpreted at a microscopic level, by comparison with the crystalline phase. [S0163-1829(98)06514-X]

I. INTRODUCTION

The achievement of a truly microscopic understanding of the dynamics of supercooled liquids and glasses still constitutes an open challenge to the condensed-matter sciences. While significant advances have been made in the elucidation of the origin of ''glassy phenomena'' in idealized systems,[1] a widely accepted model providing a comprehensive picture of these dynamic phenomena has yet to be developed. The need for a molecular-scale version of the formalisms available at present to describe the dynamics of deeply supercooled liquids and glasses is evident, and extensions of current mode-coupling (MCT) approaches which include the effects of molecular rotations are now underway.[2] Such efforts stem from the need to account for the intricacies found in the dynamics of materials which can be prepared in the glass form (i.e., the need of quantifying the effect of molecular rotations on quantities amenable to experiment, the effect of couplings between collective and molecular degrees of freedom on experimentally accessible quantities such as mean-square-displacements, etc.). In other words, they are dictated by the absence (colloidal suspensions may perhaps constitute an exception[3]) of physical systems whose dynamic behaviors can be described in detail by formalisms suitable for hard or Lennard-Jones spheres.

Glycerol is perhaps the most widely studied liquid used as a testing-ground for most theories or rationalizations about the mechanisms underlying the liquid-glass transition. Its high viscosity at the freezing point ($\approx$3 Pa s close to T_m=291 K) makes nucleation into crystallites highly unlikely, thus enabling the supercooled liquid (SCL) to be explored by a wide variety of techniques.[4–9] However, and contrary to what could be expected, examination of the relevant literature does not lead to any firm conclusion about the main details of the dynamics at microscopic scales within the liquid, SCL or glass phases. As an example, let us consider some of the NMR studies.[5] There it is found that some of the reported estimates for transport and dynamic quantities such as the self-diffusion coefficient $D_T(T)$ or the reorientational correlation time show wild variations depending upon the particular experimental technique employed. More specifically, let us consider first the isotopic-dilution studies of Kintzinger and Zeidler[5] alongside with estimates of the self-diffusion coefficient derived by pulsed-field-gradient NMR or Mössbauer scattering.[5,9] The former reports correlation times for molecular rotations and translational diffusion which are of comparable magnitude. The derived self-diffusion coefficients are then far larger than those derived from the latter set of experiments, which on the other hand are better suited for the determination of macroscopic mass-difussion constants. Similar remarks apply to results concerning the mechanisms of molecular reorientations. New NMR techniques, such as the hole-burning experiments of Kuhns and Conradi,[5] portray molecular rotations as taking place by means of large-angle excursions, whereas the opposite is found in the spin-alignment experiments of Diehl *et al.*[5]

Additional interest for carrying an in-depth study on this material, is provided by tests of the predictions made by MCT approaches, some of which have been carried out using this sample.[10,11] The referred comparisons between measurement and the MCT prediction rely on a number of assumptions before proceeding with the usual scaling analysis.[10,11] In particular, (a) the vibrational dynamics at temperatures close to the glass-transition temperature T_g=185 K or at frequencies above some 10 meV are assumed to behave har-

monically, (b) no molecular modes contribute to the low-frequency spectrum, (c) the spectral shape is independent of the temperature (time-temperature superposition principle), and (d) all the relevant dynamic processes are characterized by a single relaxation time, which has the same temperature dependence as that associated with the macroscopic shear viscosity $\tau \propto \eta_s(T)/T$. Some of these assumptions may seem reasonable if a very restricted range of frequencies (or temperatures) is considered. Others are however in stark contrast with previous results from Raman spectroscopy for glycerol in crystalline and glass forms, as well as incoherent[12] (INS) and coherent[13] (CNS) inelastic neutron-scattering measurements for the glass. Clear departures from harmonic behavior were evident[12] from analysis of the temperature dependence of the low-frequency crystal Raman spectra, as well as from the temperature variation of the $Z(\omega)$ generalized frequency distributions (vibrational density of states) for the glass.

To help lifting some of the inconsistencies mentioned above, a set of neutron experiments for the crystalline, glass, and liquid phases was performed to (a) provide the first measurement of the $Z(\omega)$ vibrational frequency distribution of the crystal, thus setting an absolute scale of frequencies for this material, (b) check the validity of the molecular model described in Ref. 12 against such vibrational density of states, (c) study in detail the temperature dependence of $Z(\omega)$ for the crystal and glass, with special emphasis on the temperature dependence of the spectral shape, and (d) study in some detail the quasielastic region of the spectrum of the glass and SCL, aiming to reconcile recent results[10] with those reported previously.[4]

Our purpose here is therefore to contribute towards the rationalization of the large amount of data currently available for this important material into a consistent framework. Previous experience with other glass-forming materials[14] tells us that the generalized frequency distributions (densities of states), derived by either scattering or simulation, provide a key to unambiguously understand the origin of some features appearing in spectra measured by a variety of techniques. In the above cited case, it was possible to assign the high-frequency part of the dielectric function of a glass former, showing a strong deviation from Debye behavior (a β relaxation), to some underlying microscopic motions of mostly rotational origin. We thus expect that results derived on a fully microscopic scale may be useful to explain the origin of the reported deviations of the measured dielectric susceptibility of this material from the standard (Kohlrausch or Havriliak-Negami) line shapes[15] (a breakdown of the time-temperature superposition principle).

II. EXPERIMENTAL DETAILS

The data reported here correspond to three sets of measurements. Inelastic scattering measurements, covering a large range of energy-transfers but still achieving a fairly high energy-resolution, $\Delta\omega \approx 90$ μeV [full width at half maximum (FWHM)] at the elastic peak, were carried out on the QENS instrument at the Intense Pulsed Neutron Source (Argonne National Laboratory). Quasielastic scattering measurements were also carried out on the same instrument using far thinner samples to reduce elastic multiple-scattering effects. QENS is an inverted-geometry crystal-analyzer spectrometer (i.e., the sample is excited by a ''white'' neutron beam, keeping fixed the final wave vector[16]). Such spectrometer configuration is specially suited for measurements at relatively low temperatures, where thermal population effects made measurements in the energy-gain (anti-Stokes) side of the spectrum at frequencies well above $k_B T/\hbar$ close to impracticable. The incident neutron pulses are moderated by a solid methane moderator, providing a large spread in incident energies and the final wave vector corresponds to an energy $E_f = 3.65$ meV. The spectrometer is equipped with three detector banks mounted on a rotatable table. A single configuration was used for the inelastic measurements which provided spectra at three different angles, whereas up to nine angular ranges were covered in the quasielastic measurements. High-resolution $\Delta\omega \approx 0.9$ μeV measurements on glassy and SCL glycerol were carried out at the Institut Laue Langevin (Grenoble, France) using the backscattering instrument IN10. The instrument was set in a configuration allowing maximal resolution in energy transfers, covering momentum transfers between 0.4 and 1.9 Å^{-1} and energy transfers of ± 8 μeV. An incident wavelength of $\lambda = 6.271$ Å was selected.

In all cases the sample consisted of fully hydrogenated anhydrous glycerol (Merck) $[C_3H_5(OH)_3]$, with a stated water content not higher than 0.2%. The crystals were grown following the procedure employed previously[12] and were held in aluminum-foil sachets, which in turn were inserted in cylindrical aluminum cans of 1 cm of diameter for the inelastic studies. A similar procedure was followed by the glass, which was prepared by a quench from the liquid. The quasielastic scattering experiments employed containers with a sample thickness below 0.1 mm. Experiments on IN10 were carried out using a plate sample of 0.5 mm sample thickness.

The derivation of the $Z(\omega)$ frequency distributions involved: (a) an angular average over the three detector groups, (b) the subtraction of the contribution from the empty container, (c) the removal of the residual elastic contamination at low frequencies (below 0.15 meV) and extrapolation to zero frequency by a $\propto \omega^2$ law, (d) the estimation of a multiphonon excitation following the procedure described in Ref. 13 and subtraction of this contribution to the total spectrum, and finally, (e) the normalization to an absolute scale as it is discussed below.

The quasielastic broadening detected on IN10 on a few μeV scale was well accounted for by a single Lorentzian plus a flat background. Such a signal appears on the QENS frequency window as an unresolved contribution to the elastic intensity, while a wider quasielastic signal which would appear as a background on the IN10 window is apparent from QENS data.

To explore the contribution of multiple-scattering (MS) processes (arising from finite sample-thickness effects) to the measured quasielastic cross section, several runs of the DISCUS (Ref. 17) code were carried out for the two spectrometer settings. As input, an $S(Q,\omega)$ representative of simple hydrodynamic diffusion (a Lorentzian with linewidth $D_T Q^2$, where Q stands for the wave vector) was employed, using for the purpose the macroscopic self-diffusion coefficients reported by Tomlinson.[5] A check on the effects of MS on the observed spectra is provided by measurements at tempera-

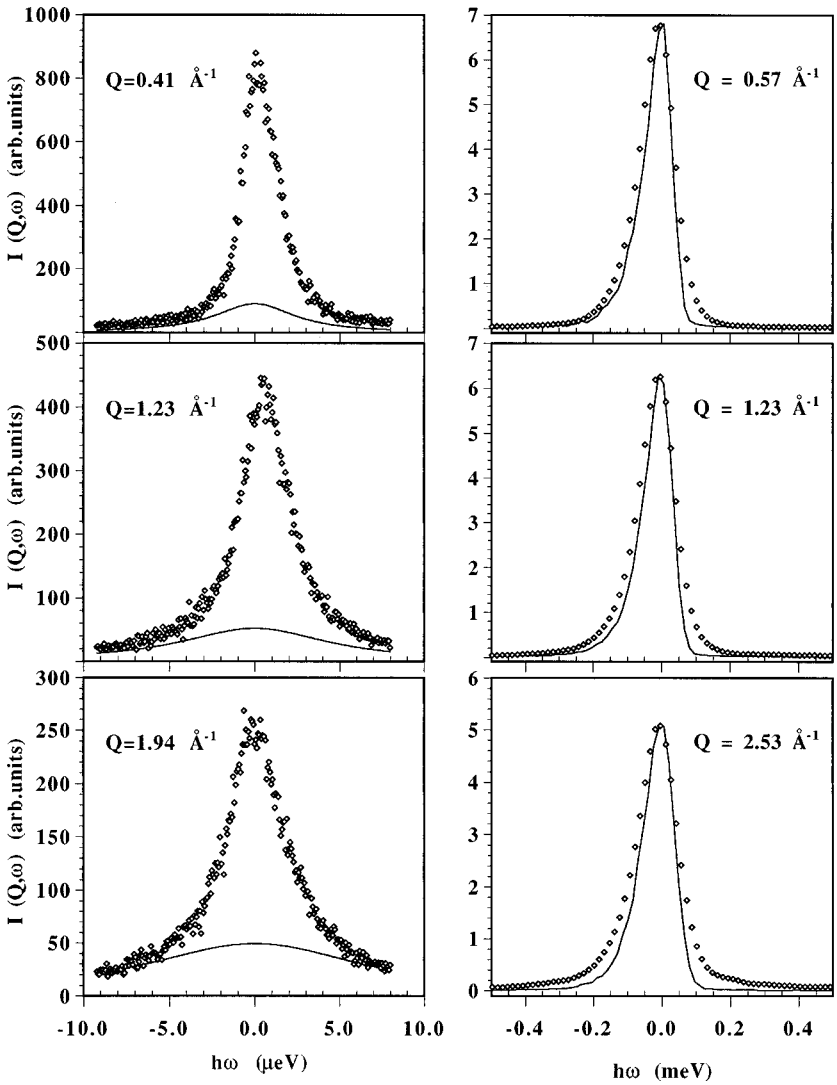

FIG. 1. Experimental spectra measured on the IN10 backscattering spectrometer (left frame) and on the QENS time-of-flight instrument (right-hand side). Symbols represent experimental data and the solid lines show the MS contributions (left) and instrumental resolution (right).

tures below 250 K, where no broadening could be observed. Under such conditions the quasielastic spectrum arises from the MS contribution only (convolved with the instrumental response), since the response is expected to be purely elastic (a δ peak). A sample of quasielastic spectra measured on both IN10 and QENS instruments is provided in Fig. 1. The importance of MS is evident as a broad component on QENS spectra, while it is only visible as a flat background on IN10. Such an unwanted feature substantially alters the spectral intensities, although it can be separated rather easily from the range of interest, -0.5 meV$\leqslant\omega\leqslant$0.5 meV.

III. RESULTS

A. Vibrational frequency distributions

Figure 2 shows the $Z(\omega)$ vibrational density of states for crystalline glycerol for a temperature $T=20$ K. A comparison between these data and the low-temperature crystal Raman spectrum shown in Fig. 2(a) of Ref. 12 seems of relevance within the context of discussions about the origin of the ''boson peak'' in glasses. In contrast with the crystal Raman spectrum, which below 10 meV shows two narrow peaks at 6.8 and 8.4 meV only, the neutron spectra unveils a far richer structure, showing a peak at about 5 meV, which extends to lower frequencies following a $\propto\omega^2$ law. Such a difference arises from the action of crystal Raman selection rules, which makes the lowest-frequency crystal peak to be Raman inactive. From the mode assignment reported in Ref. 12, it is known that such a feature represents the limit between the dominantly ''acoustic'' and the lowest ''optical'' atomic motions. This implies that even within the crystal, the atomic motions executed at such frequencies cannot be regarded as driven by sound-mode excitations only, and therefore it seems reasonable to expect that the same consideration should apply to the disordered state. It seems worth noting here that such characteristic crystal frequency comes fairly close to that of the ''boson peak'' maximum in the low-temperature spectra for the glass.

A comparison between the experimental $Z(\omega)$ and that calculated following lattice-dynamical procedures described in Ref. 12 is included in Fig. 2. The calculation is based on a model employing 13 degrees of freedom; that is, seven in-

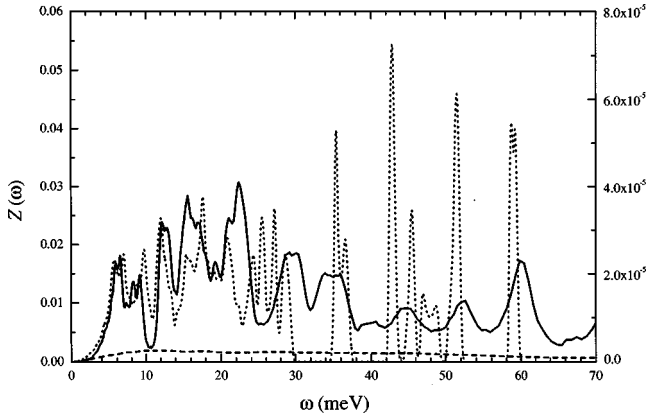

FIG. 2. The $Z(\omega,T)$ crystal frequency distribution as measured at 20 K (solid line). The calculation from lattice dynamics in the harmonic approximation following the procedures described in Ref. 12 is shown as the dotted line. The dashed line stands for the multiphonon component. Notice the different scales.

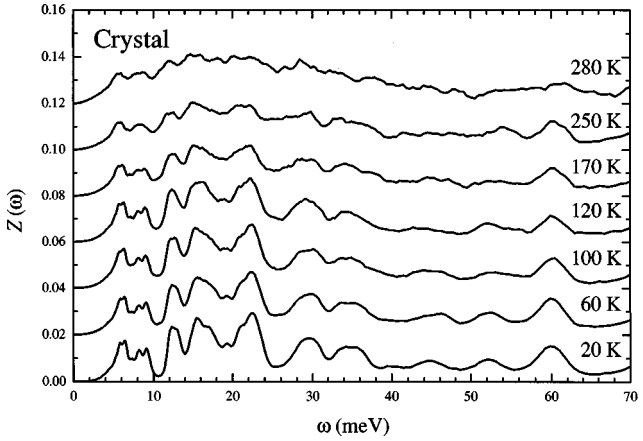

FIG. 3. The temperature dependence of the crystal spectrum. Subsequent spectra are shifted by 0.02 units upwards to enable visual comparison.

ternal molecular coordinates plus rigid-body rotations and translations. The potential parameters were refined to give adequate account of the equilibrium crystal structure, and the resulting dynamical matrix comprised a total of 49 vibrational modes. As can be seen, the calculated spectrum provides a reasonably good representation of the overall experimental frequency distribution, if finite-resolution and finite-temperature effects are taken into account. A better agreement between experiment and the harmonic dynamics calculation would require different values for the two bond-torsion force constants, as well as for the bond-bending force constants and also for the equilibrium bond angles, which were set to tetrahedral values, and also the introduction of additional force constants to allow rotation of the OH fragments. Such improvement could be achieved with ease at the expense of introducing several additional parameters to be optimized against the experimental frequencies. However, further refinements were deemed unnecessary since our main objectives in pursuing the development of this microscopic model were, (a) to quantitatively evaluate the effects of lack of a separation of time scales between the lowest frequency internal modes (bond torsions) and the set of external (lattice) vibrations, (b) to quantitatively determine the number of vibrational modes relevant at temperatures about T_g, and (c) to make this potential transferable for simulations of the fully disordered states.

The characterization of the 49 modes comprising the crystal spectrum has been discussed in Ref. 12. The study demonstrates that the close proximity of frequencies corresponding to rigid-body and bond-torsional motions makes all the vibrations with wave vectors well above the hydrodynamic limit (i.e., above a few hundredths of an Å^{-1}), to carry a strong molecular deformational component. In other words, the torsional dynamics become fully *hybridized*, so that a separation between these and the lattice modes cannot be made. This implies that the propagation of sound modes at these scales involves substantial deformations of the molecular skeleton.

To provide greater detail on the importance of anharmonic contributions to the dynamics than those allowed by our previous Raman study, the temperature dependence of the crystal spectrum up to $0.97T_m$ was monitored. A set of INS spectra covering the whole range of temperatures is shown in Fig. 3. Visual inspection of those spectra reveals that (a) the spectral shape changes steadily when the temperature is raised, losing most of the resolved structures at 280 K, (b) curiously enough, the lowest frequency multiplet structure, which extends up to about 7 meV, still persists at temperatures fairly close to melting, a behavior also revealed by our previous Raman study (one would expect larger anharmonic effects at low frequencies), and (c) the shape of the spectra becomes so complicated that individual peak-frequency shifts cannot be followed by the naked eye. The origin of such variation with temperature is better ascribed to departures from harmonic behavior, rather than to any conceivable changes in phonon dispersion, which would leave some fingerprint in the experimental specific heat. Two different effects are apparent upon inspection of Fig. 3. These regard the presence of strong effects due to finite lifetime of the excitations (spectral broadening), and the change in the curvature of the spectra due to long-wavelength (sound-mode) phonons, for frequencies below about 5 meV which follow a $Z(\omega)\propto\omega^2$ law.[18] Such an effect is quantified below in terms of the appropriate spectral frequency moments.

The relevant spectra for the glass, including two spectra for the supercooled liquid are shown in Fig. 4. Notice that, in the latter case, the frequency distribution also resembles that of the solid, since all quasielastic processes giving rise to an intercept at $\lim_{\omega\to 0}Z(\omega)$ are well below the experimental resolution, as we will see later on. The overall trend resembles the previously reported INS and CNS studies[12,13] to which the reader is referred for further details.

The normalization of the experimental $Z(\omega,T)$ spectra to an absolute scale is achieved by comparison with experimental data for the heat capacity.[19] That is, for each temperature the specific heat is calculated on a harmonic basis using the relevant distribution which is shown to vary with temperature (i.e., the calculations are performed on quasiharmonic grounds).

As discussed previously,[12] the microscopic model employing 13 degrees of freedom provides a reliable representation of the crystal dynamics up to 180 K. As shown in Ref. 12, above this temperature strong anharmonic effects cause a

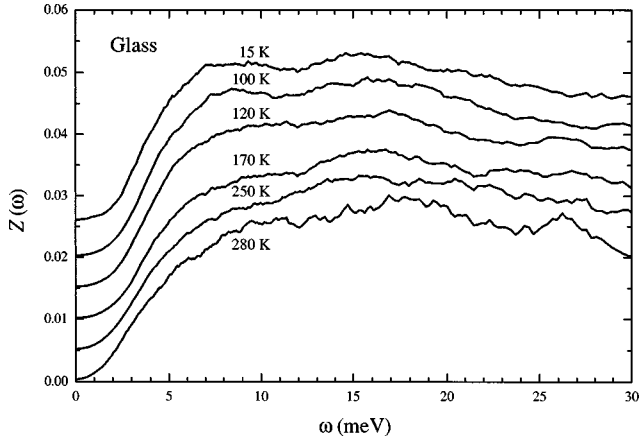

FIG. 4. Temperature dependence of the glass and SCL (280 K) frequency distributions as derived from the present INS measurements. The spectra have been upshifted by 0.05 units.

strong upwards increase of $C_p(T)$. Such a temperature thus marks the limit of validity of the quasiharmonic approximation.

From the normalized $Z(\omega,T)$ a number of quantities of importance within current discussions on glassy dynamics can be computed on quasiharmonic grounds (i.e., the calculations at each temperature are carried out using integrals over temperature-dependent distributions). This can be done safely since the measured distributions cover a range of frequencies well above $k_B T_{\max}$, that characteristic of the higher temperature here examined. To start with, the $\langle u^2(T)\rangle$ atomic mean-squared-displacements (m.s.d.), for the crystal and glass have been evaluated and their temperature dependence is shown in Fig. 5. The first remark concerns the deviation of the crystal $\langle u^2(T)\rangle$ from the far smoother behavior expected for purely harmonic motions [as an example, see Fig. 6(c) of Ref. 12]. The remarkable changes of the crystal $Z(\omega,T)$ do have a correlate in the temperature dependence of the atomic m.s.d.'s and result in a curvature of $\langle u^2(T)\rangle$, which is not so different from that followed by the glass at temperatures not too far below T_g, as is usually assumed. Furthermore, such behavior seems to be related to the strong rise in the crystal specific heat, which develops at temperatures above 250 K,[19] a temperature too low ($0.86T_m$) for premelting phenomena to develop.

An independent assessment of the reliability of our estimates for the crystal $\langle u^2(T)\rangle$ can be made by comparison with data derived directly from analysis of the Lamb-Mössbauer factors for recoilless emission reported by Champeney *et al.*[9] Their quoted value of 0.036 Å^2 at $T=280$ K compares very favorably with ours of 0.035 Å^2.

The availability of $Z(\omega,T)$ enables us to quantify the contributions of the various spectral ranges to the total $\langle u^2(T)\rangle$ displacement. Such an exercise serves to differentiate between atomic motions, which occur as a consequence of pure rigid-body displacements (i.e., from sound-mode vibrations), from others involving internal molecular motions. The lower frame of Fig. 5 displays a comparison between the percentage contribution to the atomic displacement versus the upper limit in the integral

$$\int_0^{\omega_{\max}} d\omega \, \coth\left(\frac{\hbar\omega}{2k_B T}\right)\frac{Z(\omega,T)}{\omega} \tag{1}$$

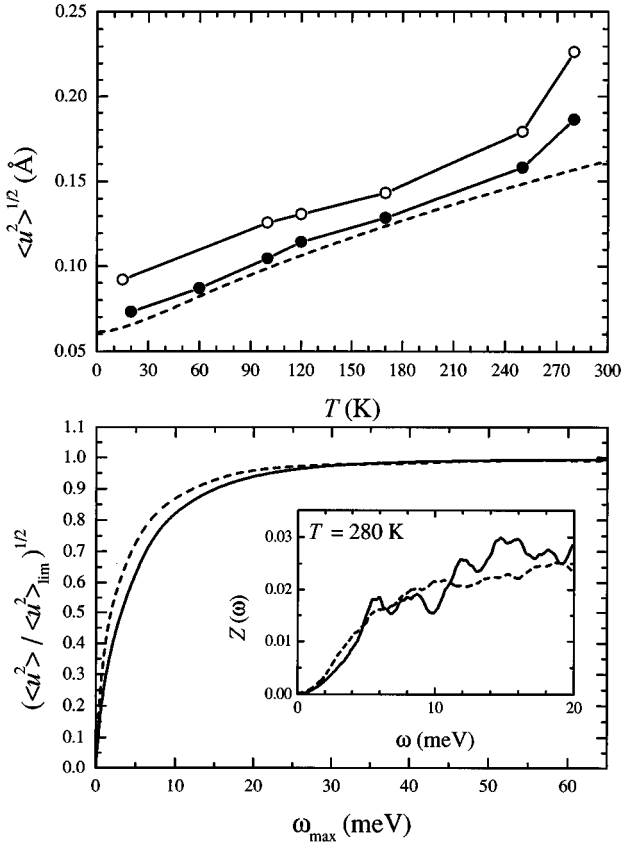

FIG. 5. The upper frame displays a comparison between the mean-squared displacements calculated from the experimental $Z(\omega,T)$ for the glass and supercooled liquid (open circles) and crystal (solid circles). The dashed line shows the prediction for a harmonic crystal calculated making use of the $Z(\omega,T=20$ K) and extrapolated to high temperatures. The lower frame depicts the dependence of the percentage contribution of the atomic m.s.d. with the upper limit of the integral taken over $Z(\omega,T=280$ K) for the crystal (solid) and supercooled liquid (dashes). The inset shows an enlargement of the low-frequency parts of the two spectra.

for the crystal and supercooled liquid at $T=280$ K. This shows that purely ''acoustic'' vibrations (i.e., those with frequencies below 5 meV) contribute to the total displacement about one half of the final value, whereas modes within the 5–10 meV range provide an additional $\approx$40% of the displacement. In other words, and as a corollary of such a finding, for a complicated material such as this, the hybridization between external and the lowest external modes will have a measurable effect in most properties measured at microscopic scales.

To quantify the importance of anharmonic effects in the glass and crystal, we have evaluated the temperature dependence of the reduced spectral frequency moments

$$\omega_D(n,T)=\left[\frac{n+3}{3}\langle\omega^n\rangle\right]^{1/n}, \tag{2}$$

$$\langle\omega^n\rangle=\int_0^{\omega_{\max}} d\omega \;\omega^n Z(\omega,T). \tag{3}$$

As evident, the 0th and -3th reduced moments are special limiting cases, and the former was calculated as[20]

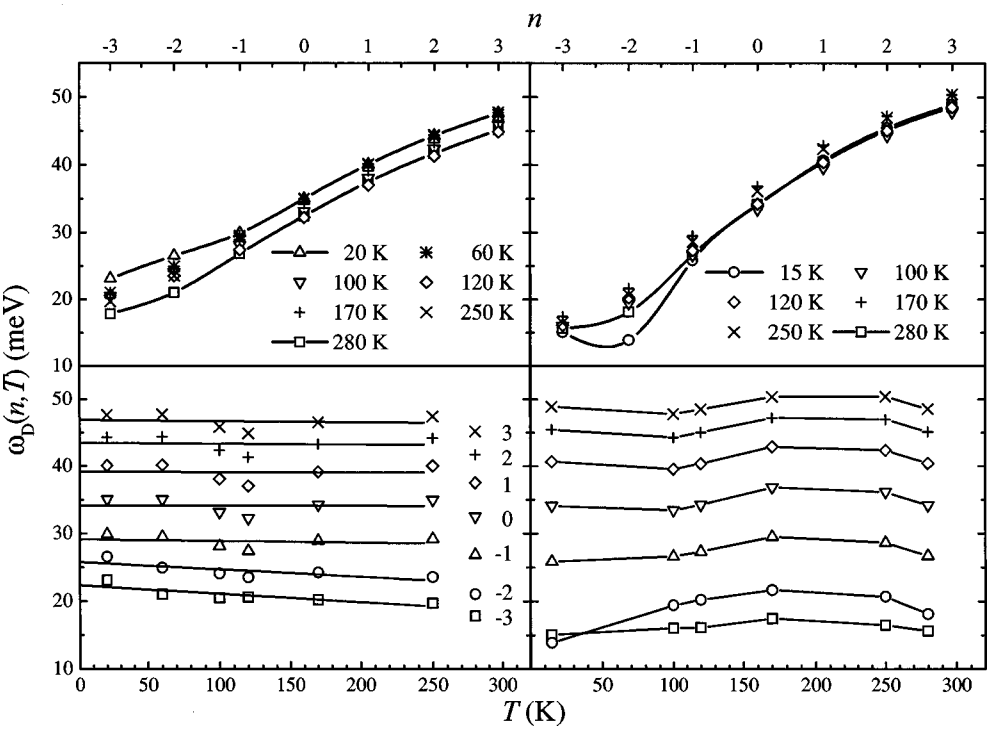

FIG. 6. The upper frame shows plots of $\omega_D(n,T)$, the reduced frequency moments, versus n for the crystal (left) and glass (right). The lower frame displays the temperature dependence of the same quantities. The solid lines represent fits to linear temperature dependences.

$$\omega_D(0,T)=e^{1/3}\exp\left[\int_0^{\omega_{\max}} d\omega \ln(Z(\omega,T))\right]\equiv\exp(\langle\ln\ \omega\rangle), \tag{4}$$

while the latter has been obtained by fitting a Debye density-of-states to the low-frequency region of the spectra. Notice that $\hbar\omega_D(-3,T=0\ \text{K})=k_B\theta_0$, where θ_0 is the low-temperature limit of the Debye temperature, a magnitude which is also accessible from low-temperature specific-heat measurements. The dependence of the $\omega_D(n,T)$ moments on the power index as well as with temperature for the glass and crystal is shown in Fig. 6. By virtue of their nature, the moments corresponding to negative powers of n, that is those weighting more heavily the low-frequency side of the spectrum, are the ones exhibiting stronger changes with temperature. The behavior with temperature of the crystal $\omega_D(n,T)$ conforms, up to 250 K, to that expected for a solid exhibiting anharmonic effects, which are weak enough to be considered as a perturbation to the harmonic ground state, that is a steady *softening* of the vibrations as the temperature is increased. The strong drop in all the moments seen at temperatures above 150 K, seems to be related to the anomalous increase in $C_p(T)$ referred to above, the origin of which is not understood at present. From the -3th moment we estimate, the orientationally averaged sound velocity for the crystal, obtaining values between 2200 ms^{-1} (280 K) and 2800 m s^{-1} (20 K). In contrast the temperature dependence of the glass frequency moments exhibits a highly nontrivial behavior. In agreement with our previous INS and CNS studies, the glass $Z(\omega,T)$ *stiffens* when the temperature is raised up to T_g, showing a substantial drop afterwards. Such counterposed behaviors may explain why, if examined over narrow time scales, the glass spectra may appear as surprisingly harmonic.[11]

A measure of the relative strength of the anharmonic component of the dynamics is provided from quantities related to the zeroth moment[21]

$$\frac{\partial\langle\ln\omega\rangle}{\partial\ln T}, \tag{5}$$

and show that the crystal spectra up to 250 K could be well accounted for with $\partial\langle\ln\omega\rangle/\partial\ln T=-1.23\times10^{-5}\text{K}^{-1}T$ up to 250 K. However, at least two different regimes seem necessary to describe the same effect for the glass: -2.5×10^{-6} estimated for $T=60$ K and -0.119 for $T=230$ K.

B. Quasielastic scattering

Measurements of the quasielastic broadening of the neutron-scattering spectra of glycerol have been repeatedly reported in the literature during the last three decades.[4] The reliability of the dynamical information coming from such measurements was put into question several times. The main difficulty concerned the relatively large values measured for the quasielastic broadenings at low momentum transfers. In a low-viscosity liquid formed by rigid particles, one expects the hydrodynamic (Fick-law) prescription $\Delta\omega=2D_TQ^2$ to hold at wave vectors of about a few tenths of an Å^{-1}, and therefore measurement of the quasielastic broadening immediately provides information on the self-diffusion coefficient. However, the experimentally determined linewidths for glycerol were systematically above those predicted from knowledge of the macroscopic self-diffusion coefficient.[22] In fact, the earliest measurements by neutron time-of-flight techniques reported temperature- and momentum-transfer-dependent linewidths, which were about two orders of magnitude above those calculable on Fick's-law grounds. Both

measurements, due to Râpeanu and Larsson and Dahlborg,[4] gave fairly consistent results, something which seems to rule out any systematic error in the measurements. The advent of a new generation of spectrometers led to a substantial improvement in instrumental resolution in energy transfer, enabling Alefeld *et al.*[4] to report broadenings of the order of 1 μeV at about $Q=1.4$ Å^{-1} and 300 K, which are still one order of magnitude above the hydrodynamic values.

More recent reports[10,11] refer to experimental setups which do not enable the monitoring of linewidths below ≈ 1 μeV. We thus carried out two sets of experiments employing different spectrometers to explore the dynamics at the μeV (IN10) and ≈ 100 μeV (QENS) scales. The same anhydrous glycerol sample has been used in both measurements, so that the uncertainty arising from different water contents is avoided.

The dependence with wave vector squared of the quasielastic linewidths measured on IN10 for all temperatures, where some broadening could be measured, is depicted in Fig. 7, together with some estimates of the widths due to hydrodynamic mass diffusion. As can be seen, no broadening was detected below 250 K, which amounts to $1.35T_g$. Also, the measured widths at the lowest explored wave vector ($Q=0.4$Å^{-1}) are above the hydrodynamic limit by an amount which strongly varies with temperature, the deviation becoming more marked as the temperature was decreased. Such results cannot be attributed to experimental artifacts such as MS since, as commented above, spectra below 250 K, where no broadenings were measured, serve to quantify the importance of this contribution. On the other hand, our previously referred estimates of the importance of MS contributions are in agreement with those of Wuttke *et al.*,[10] and show that MS effects under the present conditions would be mostly noticeable in the far end of the spectral wings, leaving unaffected the estimates for the linewidth.

The shape of the $\Delta\omega(Q,T)$ curves is reminiscent of that followed by other associated liquids such as water, showing a tendency of the linewidth to saturate at large Q values. This can be understood phenomenologically on the basis of parametric models developed some time ago,[23] which explicitly consider intramolecular proton motions. These show that under high-viscosity conditions the linewidth has the asymptotic limits

$$\lim_{Q\to 0}\Delta\,\omega(Q,T)=2[D_T+D_{rel}+D_{mix}]Q^2=2D'Q^2, \quad (6)$$

$$\lim_{Q\to\infty}\Delta\,\omega(Q,T)=2\left[\frac{1}{\tau_{00}}+\frac{2}{3}D_oQ^2\right], \quad (7)$$

where D_T is the self-diffusion coefficient, D_{rel} is a quantity which measures the motion of the atom which scatters the neutron (i.e., dominantly hydrogen) with respect to the molecular center-of-mass (c.o.m.), and D_{mix} is an admixture term between motions of the molecular c.o.m. and vibrational motions relative to it.[23] Notice that D_{rel} will then include all motions arising from the lowest frequency internal molecular modes, whose importance was verified in the previous section when considering the values of the atomic m.s.d's. The model accounts for motions which are characterized by a τ_0 residence time where nuclei vibrate about a

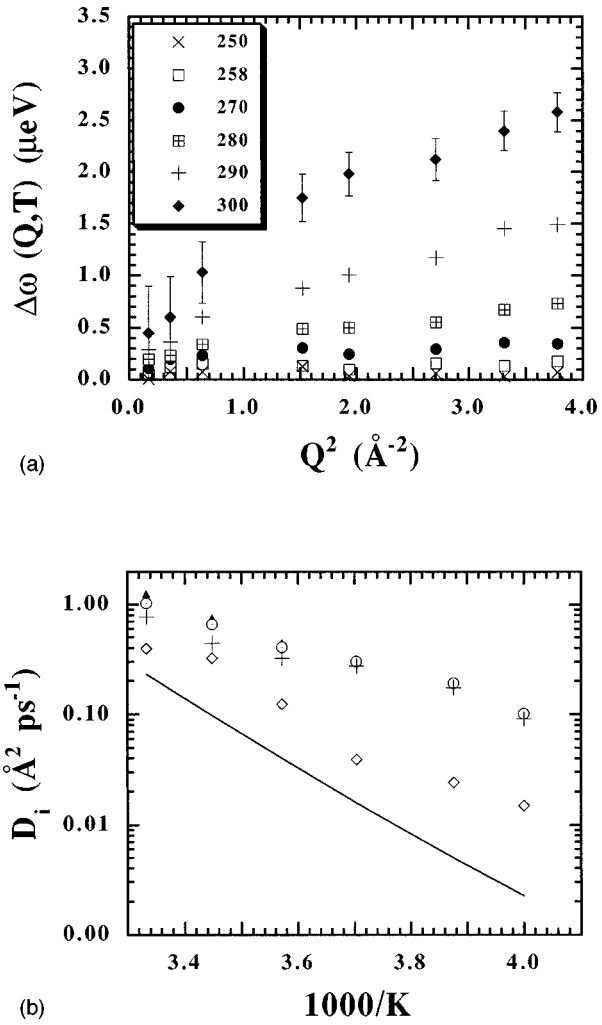

FIG. 7. (a) Quasielastic line broadenings (FWHM) as measured on IN10, for temperatures shown in the inset (in K). (b) The temperature dependence of the relaxation time as well as the different diffusion coefficients (see text). Triangles depict the D' effective diffusion coefficients, the circles stand for $D_{rel}+D_{mix}$, the crosses show D_{mix}, the diamonds stand for the reorientational diffusion constant D_o and the solid line shows the dependence with temperature of the self-diffusion coefficient D_T for which data were taken from Tomlinson (Ref. 5).

''quasiequilibrium'' position with respect to the c.o.m., changing to another position at τ_1. The latter in turn vibrates for a period τ_0' and then diffuses with a coefficient which should equal the macroscopic value D_T and finally $\tau_{00}^{-1}=\tau_0^{-1}+\tau_1^{-1}$. The above equations show that estimates for the τ_{00} time and for the constant D_o, which is associated with the reorientational motions can be derived from the slope and intercept of the tangent $d\Delta\omega/dQ$ for large Q's. Also, the value of the effective diffusion constant D' can be obtained from the low-Q slopes of $\Delta\omega(Q,T)$, thus enabling a direct comparison between contributions to the broadening arising from self-diffusion and others due to molecular, low-frequency dynamics. A comparison of the temperature dependence of the several quantities discussed above is also shown in Fig. 7. Two conclusions seem clear from this figure. The first regards the dominant contributions from molecular rotations and internal, low-frequency motions to the

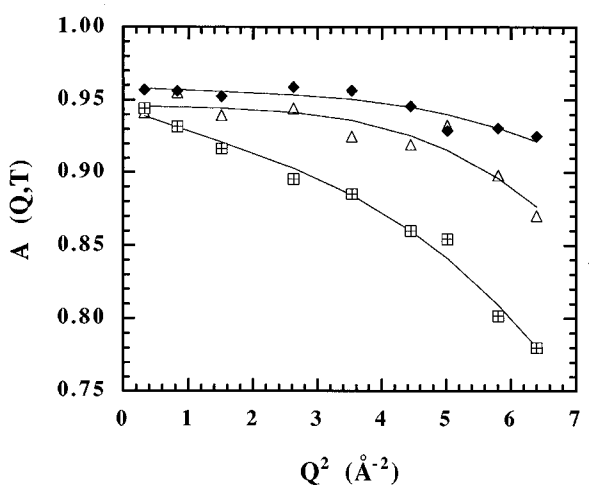

FIG. 8. Elastic incoherent structure factors for spectra measured at QENS, for temperatures $T=300$ K (squares), 290 K (triangles), and 270 K (diamonds). The solid lines are fits using Eq. (9).

observed broadening. The second concerns the somewhat milder temperature dependence exhibited by D' and D_o than that of the D_T self-diffusion coefficient, which was forced to follow the same dependence as the macroscopic shear viscosity.[10]

The set of measurements on QENS was carried out to explore whether broadenings within the meV scale are present. Indications of such quasielastic linewidths could be found in the literature,[4] as well as in recent reports[11] of time-of-flight work, where broadenings of a few hundreds of μeV are visible from the reported data. The present measurements have been able to separate a line broadening of about of 0.1 meV (FWHM) at $T=300$ K not showing any marked dependence with wave vector, as is shown in Fig. 1. Microscopically, such broadening may be ascribed to the same process described by the rotational constant $D_o(T)$ used in the analysis of the IN10 data, since its absolute value comes very close to that of 0.17 meV^2 found for this constant from the analysis of the linewidth data. To substantiate the physical soundness of such broadening (i.e., that it does not arise from MS effects) the quantities,

$$A(Q,T)=\frac{I_{\text{elast}}(Q,T)}{I_{\text{elast}}(Q,T)+I_{\text{q.el.}}(Q,T)} \tag{8}$$

are plotted in Fig. 8 for several temperatures within the SCL and normal-liquid ranges. Notice that, since all the broadenings observed on a μeV scale are not resolved here they are lumped into the I_{elast} term and consequently $A(Q,T)$ may be interpreted as an elastic incoherent structure factor. As such, the Q dependence of $A(Q,T)$ may give some hints about the underlying *geometry* of the molecular motions. The shape of the $A(Q,T)$ curves displayed in Fig. 8 serves: (a) to quantify the importance of the MS which contributes as a background of the order of 5%; this is done by inspection of the limits $\lim_{Q\to 0}A(Q,T)$, which should equal unity in the single-scattering case, (b) to unveil the contributions of microscopic motions to the spectral intensity different from rigid-body translations, and (c) to set some bounds on the distances involved in the motions being sampled, as well as their amplitudes. In this latter respect, the high-Q values of $A(Q,T)$ show that most of the motions should be ascribed to small-amplitude librational excursions since $A(Q,T)$ would otherwise show a far more pronounced decrease. To model such dynamic phenomena recourse is made to a simple physical model for isotropic librational motion of an atom around a single site[24] over the surface of a sphere of radius R with an average amplitude $\langle\theta^2(T)\rangle$. The structure factor then becomes[24]

$$A(Q,T)=\sum_{l=0}^{\infty}(2l+1)\exp[-l(l+1)\langle\theta_{\parallel}^2(T)\rangle]j_l^2(QR). \tag{9}$$

Here, $\langle\theta_{\parallel}^2(T)\rangle$ stands for the projection of the librational amplitude on the component of the wave vector in the tangential plane to the sphere, with a value which equals one half of the total amplitude, which in turn can be identified with the dimensionless quantity $D_o t$,[24] with D_o being a rotational diffusion coefficient (given in units of rad$^2 t^{-1}$). The solid lines drawn through the data in Fig. 8 are parametric fits of Eq. (9) to the data using the angular variable, the sphere radius, and a baseline subtraction to account for the MS effects as free parameters. Within the range of temperatures where clear broadenings were observed on the QENS scale, all data are compatible with motions over a sphere of radius 1.8 Å with amplitudes which increase with temperature from about 0.2 degrees at 250 K to 3.5 at 300 K. Although a unique geometric picture of such molecular motions is difficult to figure out, from knowledge of the molecular geometry such parameters seem compatible with segmental motions of the skeletal CH_2 groups about the C— C bonds. Other motions such as those of the hydroxyl O— H protons may also contribute to $A(Q,T)$ with a fractional weight of 3/8 and a geometric parameter $R\approx 1$ Å, but their presence in the measured spectra is at present difficult to assess.

IV. DISCUSSION

From data and arguments described above, the relevance of anharmonic processes for a quantitative understanding of the dynamics of crystal, glassy or SCL forms of glycerol has been demonstrated. Within the crystal, processes involving changes of the spectral distribution with temperature, contribute about 0.2% to thermodynamic functions such as specific heat at $T=170$ K (those concerning the volumic dependence of the phonons could not be evaluated because of the absence of thermal expansion and Grüneisen data). For the glass the quoted values of the same percentage contributions are about 6% of $C_p(T=170\text{ K})$ and can be taken as indicative of the importance of anharmonic effects at temperatures below (but comparable to) T_g. On the other hand, the nonmonotonic behavior of the reduced moments $\omega_D(n,T)$ as a function of temperature for the glass, provides an explanation for its apparent ''harmonic'' behavior at temperatures close to T_g. It also seems clear that such idealized behavior will not be found if a larger range of temperatures (or the corresponding frequency regions) at both sides of the maxima of $\omega_D(n,T)$ are compared.

The analysis of the quasielastic line shapes within the μeV range locates the onset of relaxational motions at temperatures close to those estimated from MCT analysis of

neutron and light-scattering data,[11] which show that structural arrest occurs at temperatures not far from 250 K. On the other hand, the present data seem to be at odds with results from other authors,[15,25] who also report scaling analyses leading to far higher values (310–320 K) for such a ''critical'' temperature.

In a NMR and quasielastic scattering study of the SCL, Wuttke *et al.*[10] report a substantial deviation of the neutron data from an average relaxation time

$$\langle \tau_Q \rangle = \int_0^{t_{\max}} dt F_s(Q,t) \tag{10}$$

determined by integration of the Fourier transform of the measured $S_s(Q,\omega)$. This lies well above the estimate $D_T^{-1}Q^2$ given by hydrodynamic diffusion, whereas within the domain of their field-gradient NMR experiment, which corresponds to wave vectors of $\approx 10^{-5}$ Å$^{-1} \leqslant Q \leqslant 10^{-3}$ Å^{-1}, such a relationship is fulfilled. Our results confirm these as well as previous neutron findings,[4] which demonstrated an excess in linewidth with respect to the hydrodynamic expectation: $\Delta\omega > D_T Q^2 (= \langle \tau_Q \rangle^{-1})$. Furthermore, the analysis of the observed quasielastic broadenings with a more realistic model than that used by previous authors, reconciles neutron, NMR, and Mössbauer scattering data.[9]

The analysis presented here provides a microscopic explanation for the origin of the discrepancy referred above, which has not been observed in far less viscous liquids.[23] In fact, as illustrated by results shown in Fig. 5, not only c.o.m. and rotational motions contribute significantly to the spectral quantities at time-length scales amenable to measurement by neutron scattering, but also those arising from molecular internal low-frequency motions.

To draw a more microscopic picture of the dynamics of this material, recourse is made to the crystal dynamics results described in more detail in Ref. 12. From examination of the mode eigenvectors corresponding to the set of 49 normal modes which comprise the relevant low-frequency dynamics,[12] a number of conclusions are drawn, which seem relevant to understand the nature of atomic motions in the glassy and supercooled-liquid states. First regards the difficulty of having pure rigid-body rotations or c.o.m. motions (in such highly viscous and highly bonded media). As expected from the relatively low values of the free-molecule bond-torsion frequencies,[12] within the condensed phases the molecule retains a substantial flexibility, which makes pure rigid-molecule motions highly unlikely. Indeed, the crystal mode eigenvectors[12] show that all of the normal-mode motions are highly hybridized, or in other words, any motion of the whole molecule will cost less energy if, instead of rotating or displacing the molecule as a rigid unit, it deforms itself by means of internal-rotation motions (torsions). This happens as a consequence of the fact that such motions will: (a) take place within a smaller volume and (b) in doing so, some of the hydrogen bonds anchoring the particle to its nearest neighbors do not have to be severed to allow such motion. Only at very low wave vectors (below $\approx 10^{-2}$ Å^{-1}) can these motions become uncoupled and only then is a separation of translations, rotations, and molecular internal motions possible.

Another conclusion can be drawn, regarding the assumption usually made in scaling analyses[25] that vibrations and relaxations can be treated as independent degrees of freedom. This is brought to the fore to justify the subtraction of the spectral part comprising the ''boson peak'' (a region which in this material stretches from about 0.5 up to 6 meV) from the measured susceptibility [i.e., $\chi(\omega)'' = \omega S(Q,\omega)/k_B T$] in order to fit the susceptibility minimum to the MCT predictions, and derive estimates for a critical temperature T_c. Application of this data treatment steps lead to estimation of such temperature some 60–70 K above that of 250 K mentioned in previous paragraphs.[25] It is worth remarking here, that having internal molecular modes with frequencies comparable to others involved in collective motions (hybridization) is expected to give rise to highly nontrivial behaviors. This is best demonstrated by results for this,[12] as well as other glass-forming material,[26] which show that such admixture of modes results in a $Z(\omega)$ spectral distribution which covers frequencies *above and below* those corresponding to the rigid-molecule solid. Since the effect of hybridization persists at scales down to at least 0.1 Å^{-1} and 1 μeV, the overestimation reported in Refs. 11,25 of the temperature of structural arrest could have well arisen from the fact that the ''vibrational'' frequency distribution, at temperatures comparable with T_g or above, a substantial portion of the frequency spectrum extends to frequencies well below the ''boson peak.'' This would then hamper a separation of time scales between the two kinds of motions (if relaxations can be conceived as having a different nature than vibrations), since the susceptibility well below such peaks is usually interpreted as arising from relaxations.

The third conclusion concerns the adequacy of describing all the microscopic dynamics within the liquid with only one parameter for an average relaxation time, which has the same temperature dependence as the shear viscosity. Within the range of temperatures where the dynamics of the SCL can be followed by neutron scattering (above 250 K), the self-diffusion coefficient follows an Arrhenius behavior $\ln D_T = D_{T0} \exp(\alpha 1000/T)$ with an exponent $\alpha = -6.95$. Rotational motions as characterized by D_o show a milder temperature dependence given by an exponent of -5.30, and the ''effective'' diffusion coefficient D' shows an even milder dependence as given by an exponent $\alpha = -3.54$. This arises as a consequence of the terms different from D_T in Eq. (6) having a far weaker temperature dependence than that of self-diffusion. This is easily understood since D_{mix} contains contributions arising from mostly harmonic segmental motions. A behavior mimicking the present results was also found for normal liquid and supercooled water,[23] where two relaxation times associated with c.o.m. motions and reorientations are needed to describe the spectra, the latter also showing an Arrhenius behavior with an activation energy far smaller than that associated with molecular translations.

In summary, the onset of ''relaxational'' motions in a highly viscous liquid composed of particles with internal energy levels, which are thermally populated at temperatures comparable to T_g, involves an interplay of internal and external dynamics which, as could be expected, lead to substantial deviations from hydrodynamic (or MCT) predictions even at wave-vector scales of a few tenths of an Å^{-1}.

Finally, the present data can also help to elucidate the origin of the deviation of the shape of the dissipative part of the dielectric spectra from a single Havriliak-Negami or Cole-Davidson line shape.[15] Fitting the high-frequency wings with an additional relaxation function, yields additional parameters showing a temperature dependence substantially different from that expected for higher-frequency ($\beta-$) relaxations. The process being sampled in these measurements extends over the μeV range also explored in this work. It could then be sensibly expected that the origin of such an apparent anomaly arises from the lack of time-scale separation between rototranslational and molecular deformation movements, which would result in a relaxation pattern showing such anomalous dependence with temperature.

ACKNOWLEDGMENTS

Work supported in part by DGICYT (Spain) Grant No. PB95-0075-c03-01. Dr. O. Randl of the Institute Laue Langevin is acknowledged for the help given during the measurements at the IN10 spectrometer. The work at ANL was supported by the U.S. Department of Energy, BES-Materials Sciences, under Contract No. W-31-109-ENG-38.

[1] See W. Götze, in *Liquids, Freezing and the Glass Transition*, edited by J. P. Hansen *et al.* (North-Holland, Amsterdam, 1991), p. 287; for the ''standard'' version of the kinetic (''mode-coupling'') theory. For the appearance of ''glassy phenomena'' in ordered systems see, for instance, P. Chandra *et al.*, Phys. Rev. Lett. **76**, 4805 (1996); L. M. Floría *et al.*, Adv. Phys. **45**, 505 (1996).

[2] R. Schilling *et al.* (unpublished).

[3] P. N. Pusey, in *Liquids, Freezing and the Glass Transition* (Ref. 1), p. 765.

[4] S. Râpeanu, Phys. Lett. **28A**, 31 (1968); K. E. Larsson and U. Dahlborg, Physica (Amsterdam) **30**, 1561 (1964); B. Alefeld, M. Birr, and A. Heidemann, Naturwissenschaften **56**, 410 (1969); M. Birr, Z. Phys. **238**, 221 (1970).

[5] N. Bloembergen, E. Purcell, and R. Pound, Phys. Rev. **73**, 679 (1948); J. P. Kintzinger and M. D. Zeidler, Ber. Bunsenges. Phys. Chem. **77**, 98 (1972); P. L. Kunhns and M. S. Conradi, J. Chem. Phys. **77**, 1771 (1982); R. M. Diehl, F. Fujara, and H. Sillescu, Europhys. Lett. **13**, 257 (1990); F. Fujara *et al.*, *ibid.* **14**, 563 (1991); D. J. Tomlinson, Mol. Phys. **25**, 735 (1972). For a recent review on these topics, see E. Rössler and M. Taupitz, in *Disorder Effects in Relaxational Processes*, edited by R. Richert and A. Blumen (Springer, Berlin, 1994), p. 361.

[6] N. Menon and S. R. Nagel, Phys. Rev. Lett. **74**, 1230 (1995), and references therein.

[7] Y. H. Jeong, Phys. Rev. A **36**, 766 (1989); Y. H. Jeong, S. R. Nagel, and S. Bhattacharya, *ibid.* **34**, 602 (1986).

[8] R. S. Miller and R. A. MacPhail, J. Chem. Phys. **106**, 3393 (1997); E. Rössler *et al.*, Phys. Rev. B **49**, 14 967 (1994); S. Kojima, *ibid.* **47**, 2924 (1993).

[9] D.C. Champeney and D.F. Sedgwick, J. Phys. C **5**, 1903 (1972); D. C. Champeney and F. W. D. Woodhams, J. Phys. B **1**, 620 (1968); M. Elwenspoek, M. Soltwisch, and D. Quitmann, Mol. Phys. **35**, 1221 (1978); G. U. Nienhaus *et al.*, Phys. Rev. B **43**, 3345 (1991).

[10] J. Wuttke *et al.*, Phys. Rev. E **54**, 5364 (1996).

[11] J. Wuttke, W. Petry, and S. Pouget, J. Chem. Phys. **105**, 5177 (1996); J. Wuttke *et al.*, Phys. Rev. Lett. **72**, 3052 (1994).

[12] F. J. Bermejo *et al.*, Phys. Rev. B **53**, 5259 (1996). Tables of mode-eigenvector components are available as AIP document no. PAPS: PRMDO-53-5259-3. Order by PAPS number and journal reference from American Institute of Physics, Physics Auxiliary Publication Service, Carolyn Gelbach, 500 Sunnyside Boulevard, Woodbury, New York, 11797. Fax: 516-576-2223, e-mail:paps@aip.org. The price is $1.50 for one microfiche or $5.00 for photocopies. Airmail additional. Make checks payable to the American Institute of Physics.

[13] J. Dawidowski *et al.*, Phys. Rev. E **53**, 5079 (1996).

[14] F. J. Bermejo *et al.*, J. Non-Cryst. Solids **172**, 167 (1994).

[15] A. Schönhals *et al.*, Phys. Rev. Lett. **70**, 3459 (1993). Also, A. Hofman *et al.*, in *Disorder Effects in Relaxational Processes* (Ref. 5), p. 309.

[16] C. G. Windsor, *Pulsed Neutron Scattering* (Taylor and Francis, London, 1981), Chap. 9, p. 331.

[17] M. W. Johnson, AERE Report No. 7682, 1974 (unpublished).

[18] See, for instance, S. W. Lovesey, *Theory of Neutron Scattering from Condensed Matter* (Oxford Science, New York, 1986, p. 124). In all real materials each phonon frequency $\omega(Q)$ is renormalized by weak anharmonic interactions resulting in $\Omega(Q,T)=\omega(Q)+\Delta(Q,T)+i\Gamma(Q,T)$ where Δ stands for the shift from the noninteracting phonon frequency and Γ is the inverse of the lifetime. An evaluation of Δ,Γ is beyond reach since it requires knowledge of the cubic and quartic interaction coefficients. A simple model would assign to the shift a value which makes the bare frequency renormalized by $(1-3\gamma\alpha_l)$, where γ stands for the macroscopic Grüneisen constant and α_l for the linear expansion coefficient. It would also predict a linear temperature dependence for the shift and damping terms for temperatures well above the Debye temperature of the solid.

[19] The data used for comparison of the calculated and measured heat capacity are those of G. E. Gibson and W. F. Giauque, J. Am. Chem. Soc. **45**, 93 (1923), M. Rajeswari and A. K. Raychauduri, Phys. Rev. B **47**, 3036 (1993); R. S. Craig *et al.*, J. Appl. Phys. **36**, 108 (1965).

[20] See, for instance, T. H. K. Barron *et al.*, Adv. Phys. **29**, 609 (1980).

[21] J. C. K. Hui and P. B. Allen, J. Phys. C **8**, 2923 (1975).

[22] Values for the diffusion coefficient as measured from NMR field-gradient techniques were taken from Tomlinson (Ref. 5).

[23] See, for instance, K. E. Larsson, Phys. Rev. **167**, 171 (1968). For recent applications see, for instance, S. H. Chen, in *Hydrogen-Bonded Liquids*, edited by J. C. Dore and J. Teixeira (Kluwer, Dordrecht, 1991), p. 289.

[24] R. E. Lechner, in *Quasielastic Neutron Scattering*, edited by J. Colmenero, A. Alegría, and F. J. Bermejo (World Scientific, Singapore, 1994), p. 62.

[25] E. Rössler, A. P. Sokolov, A. Kisliuk, and D. Quitmann, Phys. Rev. B **49**, 14 967 (1994).

[26] A. Criado *et al.*, Mol. Phys. **82**, 787 (1994).